

Published in final edited form as:

J Mol Cell Cardiol. 2012 September ; 53(3): 437–445. doi:10.1016/j.yjmcc.2012.07.001.

Cardiac specific ATP-sensitive K⁺ channel (K_{ATP}) overexpression results in embryonic lethality

Amir Toib^{1,3}, Hai Xia Zhang^{2,3}, Thomas J. Broekelmann², Krzysztof L. Hycr^{3,4,5}, Qiusha Guo², Feng Chen², Maria S. Remedi^{2,3}, and Colin G. Nichols^{2,3}

¹Department of Pediatrics, University School of Medicine, St. Louis, MO, 63110

²Department of Cell Biology and Physiology, University School of Medicine, St. Louis, MO, 63110

³Center for the Investigation of Membrane Excitability Diseases, University School of Medicine, St. Louis, MO, 63110

⁴Hope Center for Neurological Disorders, University School of Medicine, St. Louis, MO, 63110

⁵Alafi Neuroimaging Laboratory Washington, University School of Medicine, St. Louis, MO, 63110

Abstract

Transgenic mice overexpressing SUR1 and gain of function Kir6.2[ΔN30, K185Q] K_{ATP} channel subunits, under cardiac α-myosin heavy chain (αMHC) promoter control, demonstrate arrhythmia susceptibility and premature death. Pregnant mice, crossed to carry double transgenic progeny, which harbor high levels of both overexpressed subunits, exhibit the most extreme phenotype and do not deliver any *double transgenic* pups.

To explore the fetal lethality and embryonic phenotype that result from K_{ATP} overexpression, wild type (WT) and K_{ATP} overexpressing embryonic cardiomyocytes were isolated, cultured and voltage-clamped using whole cell and excised patch clamp techniques. Whole mount embryonic imaging, Hematoxylin and Eosin (H&E) and α smooth muscle actin (αSMA) immunostaining were used to assess anatomy, histology and cardiac development in K_{ATP} overexpressing and WT embryos. *Double transgenic* embryos developed *in utero* heart failure and 100% embryonic lethality by 11.5 days post conception (dpc). K_{ATP} currents were detectable in both WT and K_{ATP}-overexpressing embryonic cardiomyocytes, starting at early stages of cardiac development (9.5 dpc). In contrast to adult cardiomyocytes, WT and K_{ATP}-overexpressing embryonic cardiomyocytes exhibit basal and spontaneous K_{ATP} current, implying that these channels may be open and active under physiological conditions. At 9.5 dpc, live *double transgenic* embryos demonstrated normal looping pattern, although all cardiac structures were collapsed, probably representing failed, non-contractile chambers.

In conclusion, K_{ATP} channels are present and active in embryonic myocytes, and overexpression causes *in utero* heart failure and results in embryonic lethality. These results suggest that the K_{ATP} channel may have an important physiological role during early cardiac development.

© 2012 Elsevier Ltd. All rights reserved.

To whom correspondence should be addressed: Amir Toib, MD, Department of Pediatrics, Division of Pediatric Cardiology, St. Christopher's Hospital for Children, 3601 A Street, Philadelphia, PA 19134, Telephone: 215 – 4276804, Fax: 215 – 4278960, amir.toib@drexelmed.edu.

Publisher's Disclaimer: This is a PDF file of an unedited manuscript that has been accepted for publication. As a service to our customers we are providing this early version of the manuscript. The manuscript will undergo copyediting, typesetting, and review of the resulting proof before it is published in its final citable form. Please note that during the production process errors may be discovered which could affect the content, and all legal disclaimers that apply to the journal pertain.

Disclosures: None

Keywords

ATP sensitive K channel (K_{ATP}); Cardiac development; Heart failure; Embryonic lethality

Introduction

In the adult heart sarcolemma, K_{ATP} channels are present at higher density than any other K^+ channels although, under physiological conditions, these channels are essentially closed, and opening of as few as 1% of K_{ATP} channels is expected to shorten cardiac action potential by about 50% [1]. Opening of the K_{ATP} channel protects the heart during ischemia and reperfusion injury [2, 3] and loss of channel activity is associated with reduced cardiac stress handling, heart failure and cardiomyopathy [4–6]. Structurally, K_{ATP} channels are hetero-octameric complexes of two separate proteins: the sulfonylurea receptor (SURx) subunits and pore-forming (Kir6.x) subunits [7]. Kir6.1 (*KCNJ8*) and Kir6.2 (*KCNJ11*) are members of the inwardly rectifying potassium channel family while the regulatory subunits, SUR1 (*ABCC8*) and SUR2 (*ABCC9*), belong to the ATP-binding cassette (ABC) superfamily of membrane proteins. Different combinations of Kir6.x and SURx subunits generate tissue-specific channels [7]. In rodents, ventricular K_{ATP} is composed predominantly of Kir6.2 and SUR2A [1, 8]. Kir6.2 and SUR1 predominate in mouse atria [1], although SUR1 is also present in ventricular tissue [9, 10].

Transgenic mice overexpressing SUR1 or gain-of-function Kir6.2 mutant (Kir6.2 [Δ N30, K185Q]) under cardiac α MHC promoter control have been generated [11, 12]. Kir6.2 [Δ N30, K185Q] single transgenic (STG) mice exhibit ~40 fold reduction in ATP sensitivity combined with overexpression of the subunit of up to 400 fold [11], depending on line. SUR1 STG overexpress the SUR1 subunit by up to 100 fold [12], again depending on line. None of these STG animals exhibits an overt cardiac phenotype, other than PR prolongation in SUR1 overexpressors [11, 12]. However, cross-breeding of the two STG strains yielded SUR1-Kir6.2[Δ N30, K185Q] DTG mice that demonstrate marked arrhythmia susceptibility and premature death, even with relatively low expression of one or the other of the transgenes. Pregnant mice, crossed to carry double transgenic (DTG) progeny that harbor high levels of both overexpressed subunits, exhibit the most extreme phenotype and do not deliver any DTG pups [13].

It has previously been demonstrated that K_{ATP} channels are expressed and active, from early stages and throughout cardiac development in both mice and rats, although the physiological role and expression pattern in these early stages is not well characterized [14–18]. Here we characterized the embryonic lethality of K_{ATP} overexpressing DTG mice, showing that it is associated with *in utero* heart failure and arrest of normal cardiac development. We show that K_{ATP} channels are readily detected in WT embryos from early cardiac development stages. Together, these results indicate that K_{ATP} activity is required for normal development of the embryonic heart, and that marked over-activity of the channel can be lethal.

Materials & Methods

Generation of transgenic mice

Heterozygous STG mice overexpressing SUR1 (Line 720) or gain of function Kir6.2 [Δ N30, K185Q] (Line 4) were generated as described previously [11, 12]. All procedures complied with the standards for the care and use of animal subjects as stated in the Guide for the Care and Use of Laboratory Animals (NIH Pub. No 85-23, revised 1996). All studies were approved by the Animal Studies Committee at Washington University.

Embryonic Ultrasound Imaging

Ultrasound examination of embryos was performed using a Vevo 770 Ultrasound System (VisualSonics Inc, Toronto, Ontario, Canada). Mice were lightly anesthetized with 1.5% isoflurane in 100% oxygen by nose cone and were warmed using a heated pad and heat lamp. Physiologic parameters of adult pregnant female mice, including heart rate, respiratory rate and core body temperature, were continuously monitored by a built-in monitoring system. Maternal Heart rates ranged between 480–550 BPM. Rectal temperature was monitored, and heating was adjusted to maintain rectal temperature between 36°C and 38°C. Once anesthetized, the abdomen was shaved and further cleaned with a chemical hair remover to minimize ultrasound attenuation. Transuterine embryonic imaging was conducted in pregnant mice after surgical exteriorization of the uterus. The uterus was laid out over the maternal abdomen on a sterile gauze pad presoaked in phosphate buffered saline (PBS) at 37°C. Pre-warmed ultrasound gel was applied to the region of interest, to provide a coupling medium for the transducer. Embryos were imaged individually. Standardized imaging planes were obtained [19] and imaging was performed using 55 MHz ultrasound. Doppler flow waveforms were recorded using 40 MHz ultrasound. As reported previously, the embryonic heart was well visualized at 9.5–10.5 dpc [19]. At the end of the study, mice were euthanized by cervical dislocation while still anesthetized, and the embryos were collected for further ex-vivo studies.

Isolation and culture of embryonic cardiomyocytes

For timed mating, male and female mice were paired overnight. In the morning, the female was examined for a vaginal plug. The morning on which a mating plug was observed, was designated as 0.5 dpc. Pregnancy follow up included documentation of weight gain of the pregnant females [20]. For embryonic cell culture, pregnant females were anesthetized with Avertin administered intraperitoneally at a dose of 0.25 mg/g body weight and subsequently euthanized by cervical dislocation. The embryos were extracted from the uterus and transferred to prewarmed dissection buffer containing (in mM): 116 NaCl, 5 KCl, 0.8 MgSO₄, 1 NaH₂PO₄, 20 Hepes, and 5.5 glucose (pH 7.3). The embryonic heart was excised, cut into 2–4 pieces and placed in fresh dissection buffer with 0.5 mg/ml collagenase type 2 (Worthington) and 1.0 mg/ml Pancreatin (Sigma). After incubation for 15 min at 37°C, the tissue was mechanically dispersed, plated on polylysated glass coverslips, and incubated in DMEM supplemented with 10% fetal bovine serum at 37°C and 5% CO₂ [21].

Cellular electrophysiology

Following incubation for 24 hours, glass coverslips with adherent cells were transferred into a recording chamber. Macroscopic currents in embryonic cardiomyocytes were recorded with standard whole cell voltage-clamp recording techniques performed at room temperature. Patch-clamp electrodes (1–3 MΩ when filled with electrode filling solution) were fabricated from soda lime glass microhematocrit tubes (Kimble & Chase #2502). Cell capacitance and series resistance were estimated with a 5- to 10-mV hyperpolarizing square pulse from a holding potential (V_{hold}) of –70 mV following establishment of the whole cell recording configuration. In all whole cell experiments, current was elicited with a slow voltage ramp protocol from –120 to 40 mV over 4 s (V_{hold} = –70 mV during interpulse periods). Bath solution consisted of calcium-free Tyrode solution (137 mM NaCl, 5.4 mM KCl, 0.16 mM NaH₂PO₄, 10 mM glucose, 0.5 mM MgCl₂, 5 mM HEPES, 3 mM NaHCO₃, pH 7.3–7.4). K_{ATP} activation was assessed by addition of 100 μM pinacidil, followed by inhibition with the same solution plus 10 μM glibenclamide. Pipette solution consisted of 4 mM K₂HPO₄, 120 mM K-Aspartate, 1 mM MgCl₂, 10 mM HEPES, 20 mM KCl, 5 mM EGTA, 0.5 mM CaCl₂, and 1 mM ATP (pH 7.3). Excised inside-out patch data were obtained at a membrane potential of –50 mV. Standard bath (intracellular) and pipette (extracellular) solution used in the excised patch clamp experiments contained 150 mM KCl,

5 mM HEPES, and 10 mM EGTA (pH 7.3), with additions as noted. Data were filtered at 5 kHz. pCLAMP 8.2 software and a DigiData 1322 converter were used to generate command pulses and collect data.

Confocal imaging

The gain of function Kir6.2[ΔN30, K185Q] (Line 4) construct is tagged at the C-terminus with green fluorescent (GFP) protein [11]. Confocal images of WT and line 4 whole embryos and dissected hearts were acquired using a Zeiss LSM 5 Pascal confocal system mounted on Zeiss Axiovert 200 inverted microscope (Carl Zeiss Microimaging Inc, Thornwood, NY). To fit the specimen into the scanning area, images of embryos and dissected hearts were collected using a 2.5×/0.075 Plan-Neo lens (Zeiss) with a 1× scan zoom and 10×/0.3 Plan Neofluor lens with 0.8 scan zoom, respectively at 2048×2048 resolution. The fluorescence was excited using a 488 nm Ar laser line and collected through an LP505 filter. The images of GFP expression patterns in WT and line 4 specimens were collected under the same imaging conditions.

Histological and whole mount preparations

For histological analysis, embryos were fixed in either Bouin's solution or 4% paraformaldehyde. Embryos were processed for routine paraffin embedding, sectioned at 5 μm and stained with H&E. For immunostaining, sections were exposed to αSMA antibodies (goat anti mouse Alexa 488 secondary antibody). Whole mount images were obtained using Dark and white field microscopy to delineate embryonic heart looping pattern.

Data analysis

Cellular electrophysiology data were analyzed using ClampFit software. All statistical analyses were performed using Microsoft Excel. Results are presented as mean ± standard error of the mean (S.E.M). Statistical tests and P value or non-significance (ns) are denoted in the text and figures where appropriate.

Results

K_{ATP} overexpression results in embryonic lethality

Cross breeding of heterozygous STG mice overexpressing either SUR1 (Line 720) or gain of function Kir6.2[ΔN30, K185Q] (Line 4) yielded 20 pregnancies assessed between 9.5–18 dpc, with a total of 166 embryos. Embryonic genotyping was performed after blinded assessment of the phenotype. As expected from a heterozygous inheritance pattern of each of the single transgenes, we identified ~ 1/4 of the embryos of each genotype (WT, SUR1 STG, Kir6.2(ΔN30, K185Q) STG and DTG), with 9 % of undetermined genotype (Fig 1A). Embryonic lethality distribution and lethality percentage per pregnancy are presented in Fig 1B, C. All WT embryos were alive and appeared normal. However, ~10% of the SUR1 STG and Kir6.2[ΔN30, K185Q] STG embryos displayed embryonic lethality. Strikingly severe (85%) embryonic lethality was observed in DTG embryos, when both subunits were overexpressed at high levels. The 6/39 DTG embryos that were alive and in which the hearts were beating were detected at 9.5–10.5 dpc and no live embryos were detected after 10.5 dpc.

K_{ATP} overexpression causes *in utero* heart failure

DTG progeny were severely growth retarded at 9.5 dpc (Fig 2A), and by 10.5 dpc, demonstrated arrest of cardiac development, as well as pericardial effusion and diffuse edema (hydrops) reflecting *in utero* heart failure (Fig 2B). Ultrasound imaging of 5 pregnant females carrying DTG progeny at 9.5–10.5 dpc demonstrated WT embryos with normal

development and heart beat (Fig 2E, supplemental movie 1). DTG progeny displayed a variable phenotype: some (n = 3/12) were alive and the heart was beating (Fig 2C), some (n = 7/12) were dead and displayed pericardial effusion and diffuse edema (hydrops) (Fig 2F, supplemental movie 2) and the others (n = 2/12) were dead and absorbed (Fig 2D). Analysis of fetal heart rate of live embryos demonstrated no statistical difference between the different genotype groups (Fig 2G).

K_{ATP} currents are detected in early cardiac development

K_{ATP} channel activity was readily detected in both WT and Line 4 embryonic cardiomyocytes at 9.5 dpc. Excised inside-out patch currents demonstrated channels with 70–80 pS single channel conductance (Fig 3A) in symmetrical 150 mM K⁺, and that were inhibited by ATP, indicative of Kir6.2-dependent K_{ATP} channels. When not spontaneously detected in basal conditions, whole cell K_{ATP} currents were typically activated within 60 seconds by 100 μM pinacidil and inhibited by subsequent application of a solution containing 100 μM pinacidil and 10 μM glibenclamide (Fig 3B). Cells that demonstrated no K_{ATP} even after exposure to pinacidil for > 60 seconds were designated K_{ATP}-negative cells. Cells that did not demonstrate K_{ATP}, but were exposed to pinacidil for less than 60 seconds were designated as undetermined. Approximately 15% of WT cells (from 10 pregnancies) and 35% of Line 4 cells (from 7 pregnancies) demonstrated K_{ATP} currents (using cutoff value of <0.5 pA/pF as lack of K_{ATP}), either basally (activated immediately after breaking in), spontaneously (activated slowly before pinacidil exposure), or as a result of pinacidil activation, and confirmed by glibenclamide inhibition. Approximately 20% of WT cells and 15% of Line 4 cells were K_{ATP}-negative (according to the same criteria) (Table 1). Interestingly, in those cells that were K_{ATP}-positive, a high fraction (7/11 WT, 6/13 Line 4) demonstrated either basal or spontaneous K_{ATP} activity before pinacidil exposure (Fig. 3C).

Gain of function K_{ATP} transgene is mainly expressed in atrial tissue

In adult line 4 hearts, the GFP-tagged Kir6.2[ΔN30, K185Q] construct is highly expressed throughout the ventricular and atrial tissue as well as the pacemaker and conducting tissues [11, 22]. In contrast, confocal imaging of WT and Line 4 whole embryos and dissected hearts demonstrated prominent localization of the GFP-tagged transgene in the atria (Fig 4). This was noted in 9.5 dpc embryos (Fig 4 A, B), as well as later stage (12.5 dpc) embryos (Fig 4C). This is consistent with the pattern of expression of the driving promoter, αMHC [23] and suggests that the cardiac failure may result from K_{ATP} overactivity in this region of the embryonic heart (see Discussion).

DTG embryos demonstrate normal looping pattern at 9.5 dpc

Anatomical and histological assessment demonstrated a normal looping pattern in DTG embryos (Fig 5A). The regionalization along the cardiac tube was established and the major segments, such as the common atrium, ventricle, and outflow tract were readily identifiable at E9.5 (Fig. 5A, B). Although phenotypic variations exist among the mutants, developing cardiac cushions were visible in most embryos at this stage. However, the walls of the main chambers appeared thinner and lacking the structural strength to maintain the normal shape of the atrium, ventricle, and outflow tract. As a result, the chambers had smaller lumens and the walls appeared convoluted, leading to a collapsed appearance (Fig. 5B, C). Cardiomyocyte differentiation occurred in the DTG hearts, as evidenced by α-SMA immunostaining [24–26] (Fig 5C). These results suggest that the collapse of the cardiac structures may result from contractile failure of the chambers.

Discussion

K_{ATP} currents in the developing heart

We previously demonstrated that transgenic mice overexpressing K_{ATP} at high levels do not deliver DTG pups [13]. The present work was designed to answer the question why K_{ATP} overexpressing DTG pups are not born, as well as to explore the electrophysiological properties and functional role of K_{ATP} during heart development.

High levels of K_{ATP} current and subunit protein have been detected during early murine heart development [14, 15, 27], and it has been speculated that this may reflect a significant functional role of this current in setting the resting potential at this stage [14]. It has also been suggested that under anoxic conditions, as is typical of the fetal heart, K_{ATP} may be the dominant current maintaining the resting membrane potential, in contrast to the adult heart where IK_1 is the main hyperpolarizing current responsible for the resting membrane potential [15, 27]. K_{ATP} activation as a result of hypoxia is an established observation [28–30] and it has also been reported that hypoxia can induce an increase in transcription of the K_{ATP} subunit SUR2A [31]. The fetal circulation, which is hypoxic at baseline [32], may provide the substrate for K_{ATP} activation to fulfill a significant functional role in the embryo. In the present study we have provided further evidence that K_{ATP} currents are readily detected in the embryonic heart starting at very early stages of cardiac development.

Mechanism of embryonic lethality in K_{ATP} overexpressing mice

A key observation of this study is that K_{ATP} overexpression, controlled by α MHC promoter driven expression of highly active SUR1 and ATP insensitive Kir6.2[Δ N30, K185Q] constructs, *leads to lethality* at the onset of cardiac function. The mouse cardiac α MHC gene is activated around 7.5–8 dpc [23]. At 8 dpc, the α MHC transcript is expressed throughout the myocardium of the tubular heart (before distinct atrial and ventricular chambers form) [23]. At 9 dpc, it is detected at high levels in both the atrium and the ventricle, although decreasing in the trabeculated and outflow portion [23]. By 10 dpc α MHC mRNA continues to decrease in the trabeculated ventricle, and effectively disappearing from the ventricular tissue by 15.5 dpc [23]. Another important site of expression is in the developing sinoatrial cells that constitute the primordium of the sinus node. In DTG embryos, embryonic lethality was detected at day 9.5 dpc, with all DTG embryos dying by 11.5 dpc. The timing of lethality suggests poor cardiac function as the underlying mechanism [33]. The predominant pericardial effusion and diffuse edema also support *in utero* heart failure [34]. Prenatal ultrasound demonstrated no prolonged bradycardia or tachycardia in the live overexpressing embryos, suggesting that an undetected, acute onset and rapidly progressive process leads to lethality.

An important component of the embryonic pacing machinery is the Na-Ca exchanger (NCX). Interestingly, NCK knockout mice demonstrate a very similar phenotype to that we observed in our DTG mice, including early embryonic lethality (9–10 dpc) preceded by growth retardation and pericardial effusion, representing *in utero* heart failure. The NCX knockout phenotype appears to be the result of altered excitability and the absence of NCX in the conduction system [35, 36], consistent with a similar explanation in the DTG model.

The rationale for using a double transgenic model was to explore the extreme phenotype of K_{ATP} overexpression. Since the physiological role of this highly abundant cardiac ion channel is still unclear, the approach taken was to generate K_{ATP} overexpressing transgenic mice. This approach has previously been proven to be very efficient in discovering the role of this channel in pancreatic physiology and pathophysiology of neonatal diabetes [37].

The presumed mechanism for the embryonic lethality of the DTG embryos is K_{ATP} channel overactivity and arrest of excitability as a result of excess repolarizing current. Each of the two transgenes (Kir6.2[Δ N,K185Q] and SUR1) will contribute to enhanced channel activity in physiological conditions. (Kir6.2[Δ N,K185Q] because of reduced ATP sensitivity, SUR1 because it is more stimulated by MgADP than SUR2A [38]. Thus we conclude that the enhanced lethality of DTG than either STG (in both embryo and adult) is because of the excess K_{ATP} channel overactivity resulting from the combination of both overexpressed transgenes. It seems unlikely that the embryonic lethality is due simply to K_{ATP} channel protein overexpression, because no such phenotype was demonstrated in DTG mice highly overexpressing the Kir6.2[Δ N,K185Q] together with SUR2A at comparable levels to SUR1 in the present animals [13].

We previously reported a reduced maximal K_{ATP} current density in adult DTG (low/high combination of the subunits in contrast to the high/high combination used in this study) and STG ventricular myocytes, although we have observed no such reduction in K_{ATP} conductance in STG beta-cells expressing similar transgenes [37, 39]. It seems likely that in the adult ventricle (in which the only rigorous assessment has been made), the transgenic expressed subunits are predominantly intracellularly retained, but this appears not to be the case in beta-cells and in embryonic myocytes, since we still see high density of currents in these cells. It is possible that the patched cells are from parts of the embryonic heart with little or no expression of transgenes, but control of K_{ATP} subunit trafficking and processing is complex (e.g [40–42]), and clearly future studies are required to reach an adequate understanding of these complexities.

The pattern of expression of α MHC in the atria and developing sinus node at 9.5–11.5 dpc, reflected in the predominance of GFP fluorescence only in these regions, would suggest that the likely mechanism of lethality is excess K_{ATP} -dependent repolarizing current in the developing conduction system that leads to asystole, as a result of arrest of excitability. The collapsed chambers support the altered excitability induced heart failure hypothesis, and the demonstration of a normal looping pattern of the DTG embryos at 9.5 dpc is important in ruling out an abnormal cardiac development sequence. The phenotype severity was not uniform (some DTG embryos reached 10.5 dpc with the appropriate looping milestones, while others were already arrested and absorbed at 9.5 dpc), but this variation in timing of cardiac pathology and embryonic death may be explained by the random timing of the catastrophic arrest.

Previously, live births of single transgenic SUR1 and ATP-insensitive Kir6.2 progeny were not obviously less than wild type. However, in the present study, we took careful note of the birth ratios for all genotypes, and this clearly demonstrates that there is also some embryonic lethality in the STG progeny. This again demonstrates a variable penetrance, and can be explained by only some early embryos carrying single transgenes (but all DTG embryos) experiencing an acute heart block at this critical stage, whereas others escape this event, and hence progress to essentially normal subsequent development. The increased lethality of the STG embryos may be the result of mildly increased activity of K_{ATP} currents in these early embryonic stages, with some embryos arresting, but others surviving this critical period and then resuming essentially normal development.

Supplementary Material

Refer to Web version on PubMed Central for supplementary material.

Acknowledgments

This project was supported by NIH grants HL45742 and HL95010 (to CGN), Neuroscience Blueprint Interdisciplinary Center Core Grant P30 NS057105 (to KLH), and by T32 HL07873 (P.I. R.P. Mecham), and the Children's Discovery Institute at Washington University (to AT). We are grateful to the Mouse Cardiovascular Phenotyping Core at Washington University for help with echocardiographic studies.

Abbreviations

K_{ATP}	ATP-sensitive K ⁺ channel
αMHC	α myosin heavy chain
DTG	double transgenic
WT	wild type
H&E	Hematoxylin and Eosin
αSMA	α smooth muscle actin
dpc	days post conception
ABC	ATP-binding cassette
STG	single transgenic
PBS	phosphate buffered saline
V_{hold}	holding potential
GFP	green fluorescent protein
S.E.M	standard error of the mean
ns	non-significance
NCX	Na-Ca exchanger
UD	Undetermined
BPM	beats per minute

References

1. Zhang H, Flagg TP, Nichols CG. Cardiac sarcolemmal K(ATP) channels: Latest twists in a queuing tale! *J Mol Cell Cardiol.* Jan; 48(1):71–75. [PubMed: 19607836]
2. Kane GC, Liu XK, Yamada S, Olson TM, Terzic A. Cardiac KATP channels in health and disease. *J Mol Cell Cardiol.* 2005 Jun; 38(6):937–943. [PubMed: 15910878]
3. Zingman LV, Alekseev AE, Hodgson-Zingman DM, Terzic A. ATP-sensitive potassium channels: metabolic sensing and cardioprotection. *J Appl Physiol.* 2007 Nov; 103(5):1888–1893. [PubMed: 17641217]
4. Olson TM, Terzic A. Human K(ATP) channelopathies: diseases of metabolic homeostasis. *Pflugers Arch.* Jul; 460(2):295–306. [PubMed: 20033705]
5. Tong X, Porter LM, Liu G, Dhar-Chowdhury P, Srivastava S, Pountney DJ, et al. Consequences of cardiac myocyte-specific ablation of KATP channels in transgenic mice expressing dominant negative Kir6 subunits. *Am J Physiol Heart Circ Physiol.* 2006 Aug; 291(2):H543–H551. [PubMed: 16501027]
6. Yamada S, Kane GC, Behfar A, Liu XK, Dyer RB, Faustino RS, et al. Protection conferred by myocardial ATP-sensitive K⁺ channels in pressure overload-induced congestive heart failure revealed in KCNJ11 Kir6.2-null mutant. *J Physiol.* 2006 Dec 15; 577(Pt 3):1053–1065. [PubMed: 17038430]

7. Nichols CG. KATP channels as molecular sensors of cellular metabolism. *Nature*. 2006 Mar 23; 440(7083):470–476. [PubMed: 16554807]
8. Glukhov AV, Flagg TP, Fedorov VV, Efimov IR, Nichols CG. Differential K(ATP) channel pharmacology in intact mouse heart. *J Mol Cell Cardiol*. Jan; 48(1):152–160. [PubMed: 19744493]
9. Yokoshiki H, Sunagawa M, Seki T, Sperelakis N. Antisense oligodeoxynucleotides of sulfonylurea receptors inhibit ATP-sensitive K⁺ channels in cultured neonatal rat ventricular cells. *Pflugers Arch*. 1999 Feb; 437(3):400–408. [PubMed: 9914396]
10. Morrissey A, Rosner E, Lanning J, Parachuru L, Dhar Chowdhury P, Han S, et al. Immunolocalization of KATP channel subunits in mouse and rat cardiac myocytes and the coronary vasculature. *BMC Physiol*. 2005; 5(1):1. [PubMed: 15647111]
11. Koster JC, Knopp A, Flagg TP, Markova KP, Sha Q, Enkvetchakul D, et al. Tolerance for ATP-insensitive K(ATP) channels in transgenic mice. *Circ Res*. 2001 Nov 23; 89(11):1022–1029. [PubMed: 11717159]
12. Flagg TP, Remedi MS, Masia R, Gomes J, McLerie M, Lopatin AN, et al. Transgenic overexpression of SUR1 in the heart suppresses sarcolemmal K(ATP). *J Mol Cell Cardiol*. 2005 Oct; 39(4):647–656. [PubMed: 16099470]
13. Flagg TP, Patton B, Masia R, Mansfield C, Lopatin AN, Yamada KA, et al. Arrhythmia susceptibility and premature death in transgenic mice overexpressing both SUR1 and Kir6.2[DeltaN30,K185Q] in the heart. *Am J Physiol Heart Circ Physiol*. 2007 Jul; 293(1):H836–H845. [PubMed: 17449558]
14. Davies MP, An RH, Doevendans P, Kubalak S, Chien KR, Kass RS. Developmental changes in ionic channel activity in the embryonic murine heart. *Circ Res*. 1996 Jan; 78(1):15–25. [PubMed: 8603498]
15. Xie LH, Takano M, Noma A. Development of inwardly rectifying K⁺ channel family in rat ventricular myocytes. *Am J Physiol*. 1997 Apr; 272(4 Pt 2):H1741–H1750. [PubMed: 9139958]
16. Morrissey A, Parachuru L, Leung M, Lopez G, Nakamura TY, Tong X, et al. Expression of ATP-sensitive K⁺ channel subunits during perinatal maturation in the mouse heart. *Pediatr Res*. 2005 Aug; 58(2):185–192. [PubMed: 16085792]
17. Harrell MD, Harbi S, Hoffman JF, Zavadil J, Coetzee WA. Large-scale analysis of ion channel gene expression in the mouse heart during perinatal development. *Physiol Genomics*. 2007 Feb 12; 28(3):273–283. [PubMed: 16985003]
18. Akasaka T, Klinedinst S, Ocorr K, Bustamante EL, Kim SK, Bodmer R. The ATP-sensitive potassium (KATP) channel-encoded dSUR gene is required for Drosophila heart function and is regulated by tinman. *Proc Natl Acad Sci U S A*. 2006 Aug 8; 103(32):11999–12004. [PubMed: 16882722]
19. Pallares P, Gonzalez-Bulnes A. Non-invasive ultrasonographic characterization of phenotypic changes during embryo development in non-anesthetized mice of different genotypes. *Theriogenology*. 2008 Jul 1; 70(1):44–52. [PubMed: 18407344]
20. Mader SL, Libal NL, Pritchett-Corning K, Yang R, Murphy SJ. Refining timed pregnancies in two strains of genetically engineered mice. *Lab Anim (NY)*. 2009 Sep; 38(9):305–310. [PubMed: 19701181]
21. Stieber J, Herrmann S, Feil S, Loster J, Feil R, Biel M, et al. The hyperpolarization-activated channel HCN4 is required for the generation of pacemaker action potentials in the embryonic heart. *Proc Natl Acad Sci U S A*. 2003 Dec 9; 100(25):15235–15240. [PubMed: 14657344]
22. Dobrzynski H, Billeter R, Greener ID, Tellez JO, Chandler NJ, Flagg TP, et al. Expression of Kir2.1 and Kir6.2 transgenes under the control of the alpha-MHC promoter in the sinoatrial and atrioventricular nodes in transgenic mice. *J Mol Cell Cardiol*. 2006 Nov; 41(5):855–867. [PubMed: 16996082]
23. Lyons GE, Schiaffino S, Sassoon D, Barton P, Buckingham M. Developmental regulation of myosin gene expression in mouse cardiac muscle. *J Cell Biol*. 1990 Dec; 111(6 Pt 1):2427–2436. [PubMed: 2277065]
24. Woodcock-Mitchell J, Mitchell JJ, Low RB, Kienny M, Sengel P, Rubbia L, et al. Alpha-smooth muscle actin is transiently expressed in embryonic rat cardiac and skeletal muscles. *Differentiation*. 1988 Dec; 39(3):161–166. [PubMed: 2468547]

25. Ruzicka DL, Schwartz RJ. Sequential activation of alpha-actin genes during avian cardiogenesis: vascular smooth muscle alpha-actin gene transcripts mark the onset of cardiomyocyte differentiation. *J Cell Biol.* 1988 Dec; 107(6 Pt 2):2575–2586. [PubMed: 3204121]
26. Clement S, Stouffs M, Bettiol E, Kampf S, Krause KH, Chaponnier C, et al. Expression and function of alpha-smooth muscle actin during embryonic-stem-cell-derived cardiomyocyte differentiation. *J Cell Sci.* 2007 Jan 15; 120(Pt 2):229–238. [PubMed: 17179203]
27. Gryshchenko O, Fischer IR, Dittrich M, Viatchenko-Karpinski S, Soest J, Bohm-Pinger MM, et al. Role of ATP-dependent K(+) channels in the electrical excitability of early embryonic stem cell-derived cardiomyocytes. *J Cell Sci.* 1999 Sep; 112(Pt 17):2903–2912. [PubMed: 10444385]
28. Budas GR, Jovanovic S, Crawford RM, Jovanovic A. Hypoxia-induced preconditioning in adult stimulated cardiomyocytes is mediated by the opening and trafficking of sarcolemmal KATP channels. *FASEB J.* 2004 Jun; 18(9):1046–1048. [PubMed: 15084521]
29. Baker JE, Curry BD, Olinger GN, Gross GJ. Increased tolerance of the chronically hypoxic immature heart to ischemia. Contribution of the KATP channel. *Circulation.* 1997 Mar 4; 95(5): 1278–1285. [PubMed: 9054860]
30. Yan XS, Ma JH, Zhang PH. Modulation of K(ATP) currents in rat ventricular myocytes by hypoxia and a redox reaction. *Acta Pharmacol Sin.* 2009 Oct; 30(10):1399–1414. [PubMed: 19801996]
31. Crawford RM, Jovanovic S, Budas GR, Davies AM, Lad H, Wenger RH, et al. Chronic mild hypoxia protects heart-derived H9c2 cells against acute hypoxia/reoxygenation by regulating expression of the SUR2A subunit of the ATP-sensitive K+ channel. *J Biol Chem.* 2003 Aug 15; 278(33):31444–31455. [PubMed: 12791696]
32. Patterson AJ, Zhang L. Hypoxia and fetal heart development. *Curr Mol Med.* Oct; 10(7):653–666. [PubMed: 20712587]
33. Conway SJ, Kruzynska-Frejtag A, Kneer PL, Machnicki M, Koushik SV. What cardiovascular defect does my prenatal mouse mutant have, and why? *Genesis.* 2003 Jan; 35(1):1–21. [PubMed: 12481294]
34. Harzheim D, Pfeiffer KH, Fabritz L, Kremmer E, Buch T, Waisman A, et al. Cardiac pacemaker function of HCN4 channels in mice is confined to embryonic development and requires cyclic AMP. *EMBO J.* 2008 Feb 20; 27(4):692–703. [PubMed: 18219271]
35. Wakimoto K, Kobayashi K, Kuro OM, Yao A, Iwamoto T, Yanaka N, et al. Targeted disruption of Na+/Ca2+ exchanger gene leads to cardiomyocyte apoptosis and defects in heartbeat. *J Biol Chem.* 2000 Nov 24; 275(47):36991–36998. [PubMed: 10967099]
36. Conway SJ, Kruzynska-Frejtag A, Wang J, Rogers R, Kneer PL, Chen H, et al. Role of sodium-calcium exchanger (Ncx1) in embryonic heart development: a transgenic rescue? *Ann N Y Acad Sci.* 2002 Nov; 976:268–281. [PubMed: 12502569]
37. Koster JC, Marshall BA, Ensor N, Corbett JA, Nichols CG. Targeted overactivity of beta cell K(ATP) channels induces profound neonatal diabetes. *Cell.* 2000 Mar 17; 100(6):645–654. [PubMed: 10761930]
38. Masia R, Enkvetchakul D, Nichols CG. Differential nucleotide regulation of KATP channels by SUR1 and SUR2A. *J Mol Cell Cardiol.* 2005 Sep; 39(3):491–501. [PubMed: 15893323]
39. Remedi MS, Nichols CG. Hyperinsulinism and diabetes: genetic dissection of beta cell metabolism-excitation coupling in mice. *Cell Metab.* 2009 Dec; 10(6):442–453. [PubMed: 19945402]
40. Heusser K, Yuan H, Neagoe I, Tarasov AI, Ashcroft FM, Schwappach B. Scavenging of 14-3-3 proteins reveals their involvement in the cell-surface transport of ATP-sensitive K+ channels. *J Cell Sci.* 2006 Oct 15; 119(Pt 20):4353–4363. [PubMed: 17038548]
41. Schwappach B, Zerangue N, Jan YN, Jan LY. Molecular basis for K(ATP) assembly: transmembrane interactions mediate association of a K+ channel with an ABC transporter. *Neuron.* 2000 Apr; 26(1):155–167. [PubMed: 10798400]
42. Zerangue N, Schwappach B, Jan YN, Jan LY. A new ER trafficking signal regulates the subunit stoichiometry of plasma membrane K(ATP) channels. *Neuron.* 1999 Mar; 22(3):537–548. [PubMed: 10197533]

Highlights

- K_{ATP} currents are detected in embryonic cardiomyocytes since early stages of cardiac development.
- Embryos overexpressing K_{ATP} demonstrate normal cardiac looping pattern.
- Transgenic mice overexpressing K_{ATP} channel subunits demonstrate embryonic lethality.
- The embryonic lethality of the K_{ATP} overexpressing embryos is a result of *in utero* heart failure.

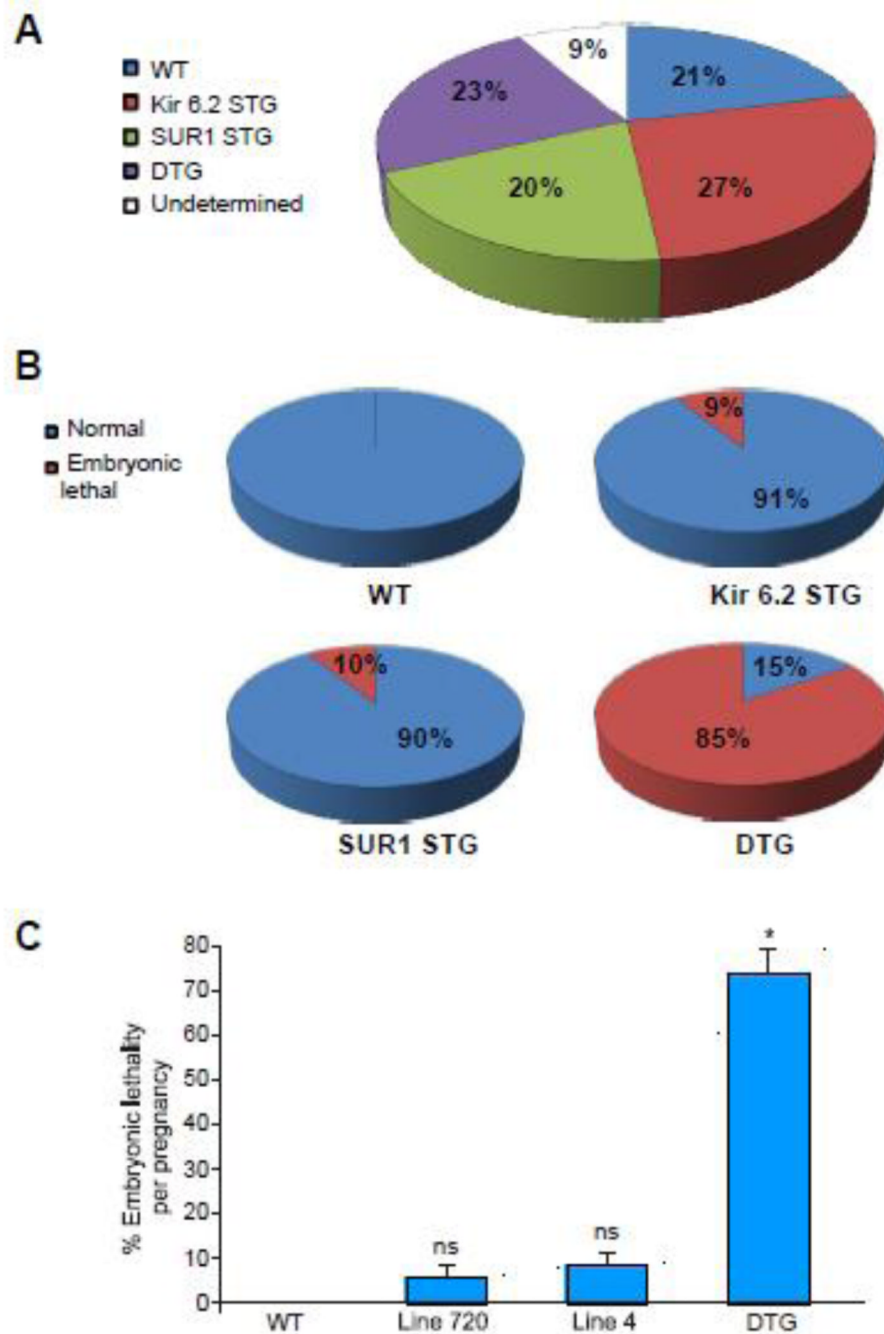


Figure 1. K_{ATP} overexpression results in embryonic lethality

(A) Genotype distribution from breeding of heterozygous STG mice overexpressing either SUR1 line 720 or gain of function Kir6.2(Δ N30, K185Q) line 4. 20 pregnancies were assessed between 9.5–18 dpc (with a total of 166 embryos). Embryonic genotyping distributed as expected from a heterozygous inheritance pattern of each of the single transgenes, with ~ 1/4 of the embryos of each genotype. (B) Embryonic lethality distribution of the different genotypes. Of note, the 15% fraction for DTG (right lower pie), represents embryos that were alive (beating heart) at 9.5–10.5 dpc, none of the DTG was alive at 11.5 dpc. (C) Embryonic lethality per pregnancy from the above crosses (* $p < 0.05$ compared to

WT, Line 720 and Line 4). No embryonic lethality was detected in 20 WT embryos. All of the DTG embryos extracted after 11.5 dpc were dead.

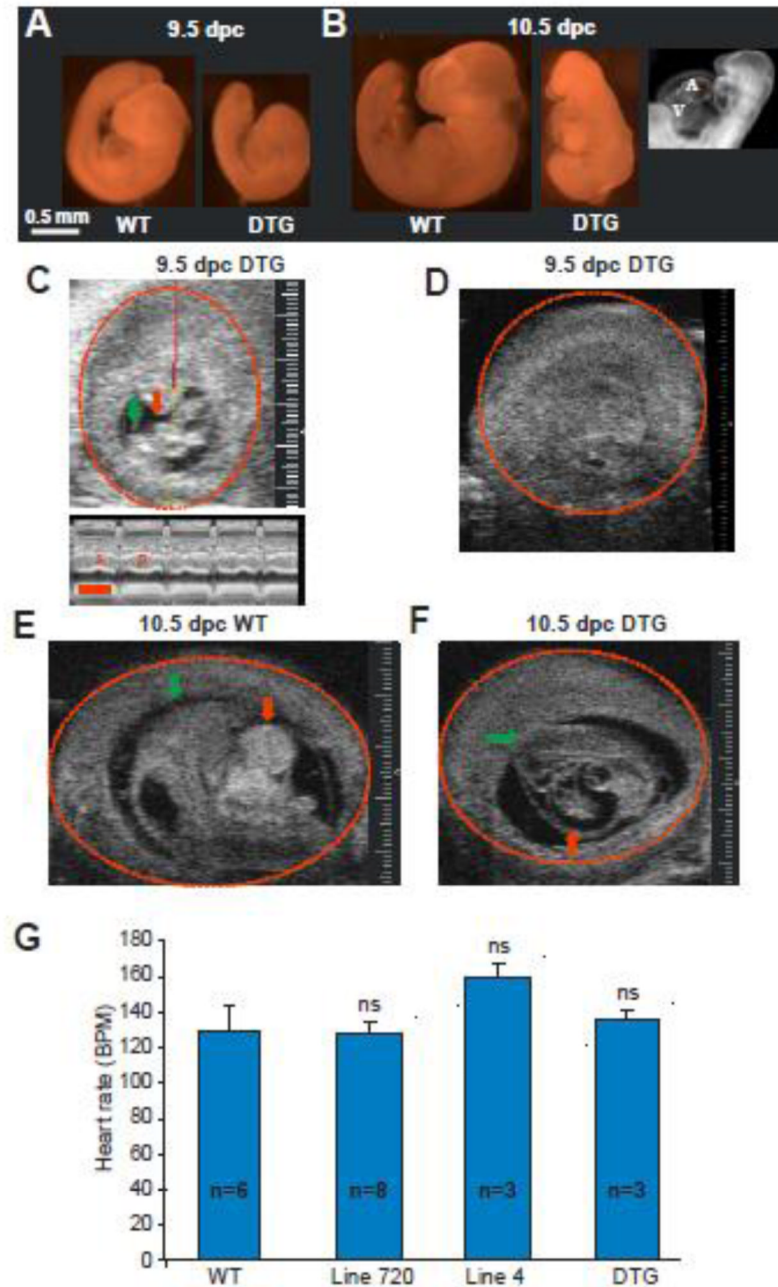


Figure 2. K_{ATP} overexpression causes *in utero* heart failure and embryonic lethality
(A) Littermate 9.5 dpc WT (left) and DTG (right) embryos. DTG embryo demonstrates growth retardation. **(B)** 10.5 dpc WT (left) and DTG (middle) embryos. DTG embryo demonstrates growth retardation, pericardial effusion and diffuse hydrops. Dark field imaging (right) demonstrates that the 10.5 dpc DTG heart is arrested developmentally at the primitive loop stage (9.5dpc). **(C)** Two dimensional ultrasound image of a 9.5 dpc live DTG embryo with a normally beating heart. The head is marked with a green arrow. The heart is marked with a red arrow. The embryonic sac is marked with a red circle. The red/yellow line represents the M mode plane across the embryo's heart. The lower M mode panel

demonstrates systole (S) and diastole (D). Sizing scale (for C–E) indicates 0.1 mm. Timing bar (red) in lower panel indicates 200 msec. **(D)** Two dimensional ultrasound of a 9.5 dpc DTG embryo, a littermate of the embryo in C, demonstrating an empty sac with an absorbed embryo. **(E)** Two dimensional ultrasound image of a 10.5 dpc WT embryo with normal development. **(F)** Two dimensional ultrasound of a 10.5 dpc DTG embryo demonstrating growth retarded embryo with pericardial effusion. **(G)** Summary of fetal heart rates (BPM=beats per minute) in live embryos demonstrates no statistical difference between the different genotype groups.

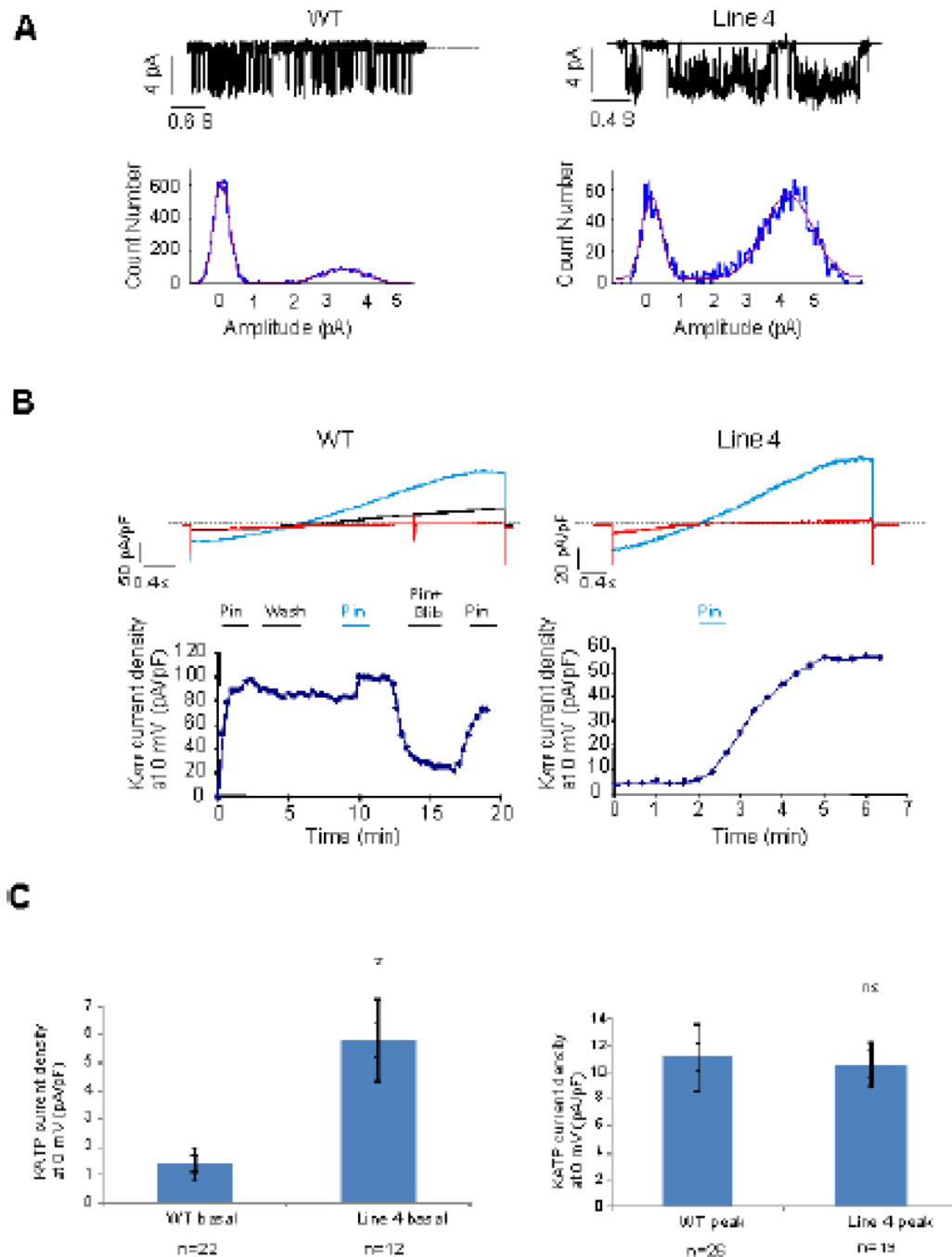


Figure 3. K_{ATP} currents are detected in embryonic myocytes throughout development
(A) Single channel K_{ATP} currents recorded in excised patches from 15 dpc WT (left) and 12 dpc Line 4 (right) ventricular myocytes. Current density histograms demonstrate 3.5–4 pA single channel current, corresponding to a 70–80 pS single channel conductance. **(B)** Whole cell voltage-clamp recordings of 12 dpc WT and 18 dpc Line 4 ventricular myocytes (Upper panels). Red: baseline current. Blue: Maximal K_{ATP} activation in presence of 100 μM of Pinacidil. Black: current in presence of 10 μM Glibenclamide and 100 μM Pinacidil. (Lower panels) K_{ATP} current versus time (Pin=Pinacidil, Glib=Glibenclamide). **(C)** Whole cell basal (left) and peak (right) K_{ATP} current density in WT and Line 4 embryonic cardiomyocytes.

Basal K_{ATP} current was significantly increased in Line 4 cardiomyocytes compared to early cardiac development WT cardiomyocytes ($p < 0.05$) No difference was noted in peak K_{ATP} current between WT and line 4 cardiomyocytes.

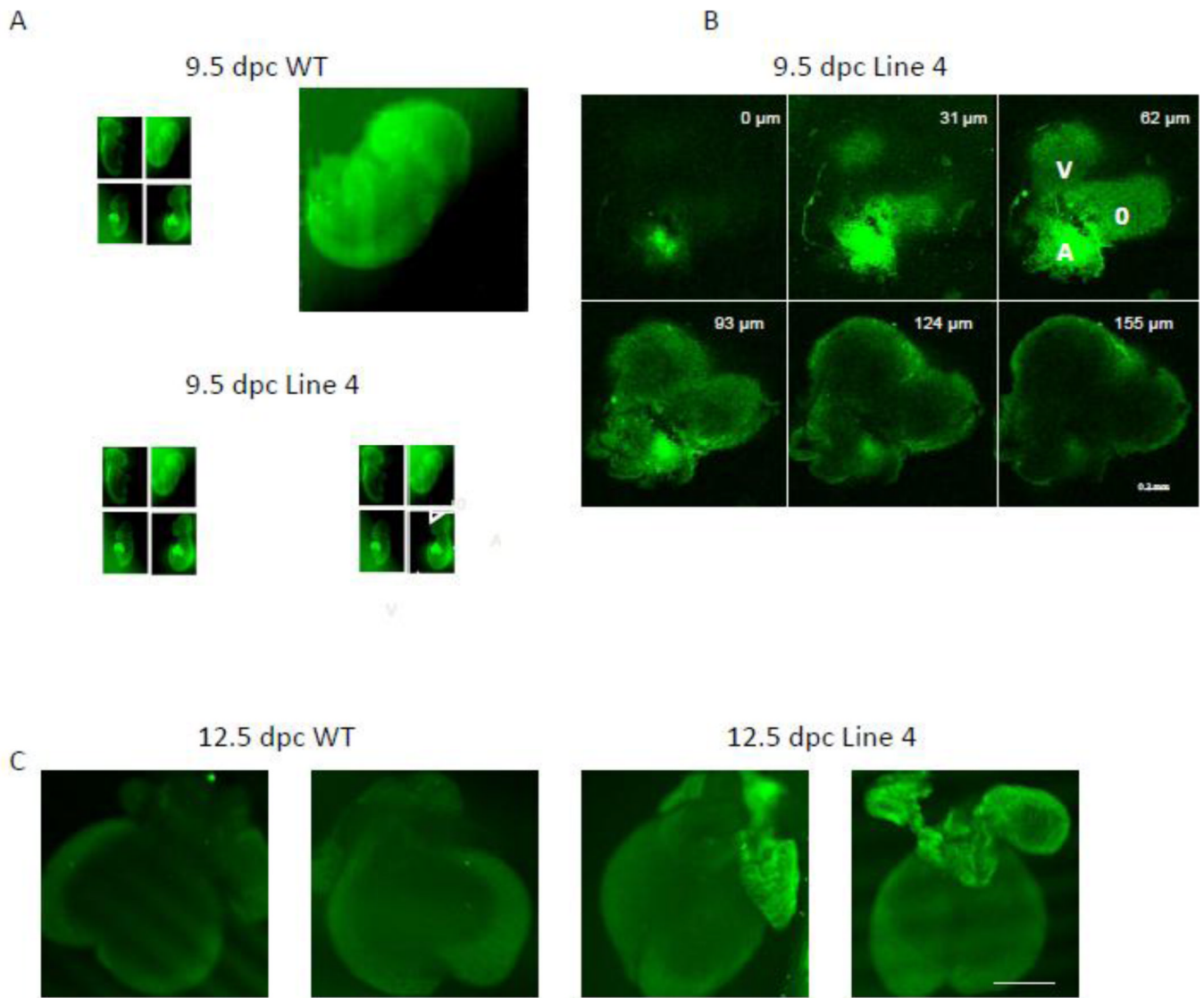


Figure 4. Gain of function K_{ATP} transgene is mainly expressed in atrial tissue
(A) Confocal images of two 9.5 dpc WT (control) littermate embryos (upper two images) and two 9.5 Line 4 littermate embryos hearts (lower 2 images). Note prominent GFP fluorescence in Line 4 transgenic mice throughout the hearts. A=atrium, V=ventricle, O=outflow. Sizing bar indicates 1 mm. **(B)** Z-sectioning (with depth information in the right upper corner of each image) confocal images of the heart from 9.5 dpc Line 4 embryo (right lower embryo in A). A=atrium, V=ventricle, O=outflow. Sizing bar indicates 0.2 mm. **(C)** Confocal images of two 12.5 dpc WT (control) littermate embryonic hearts (left 2 images) and two 12.5 Line 4 littermate embryonic hearts (right 2 images). Sizing bar indicates 1 mm.

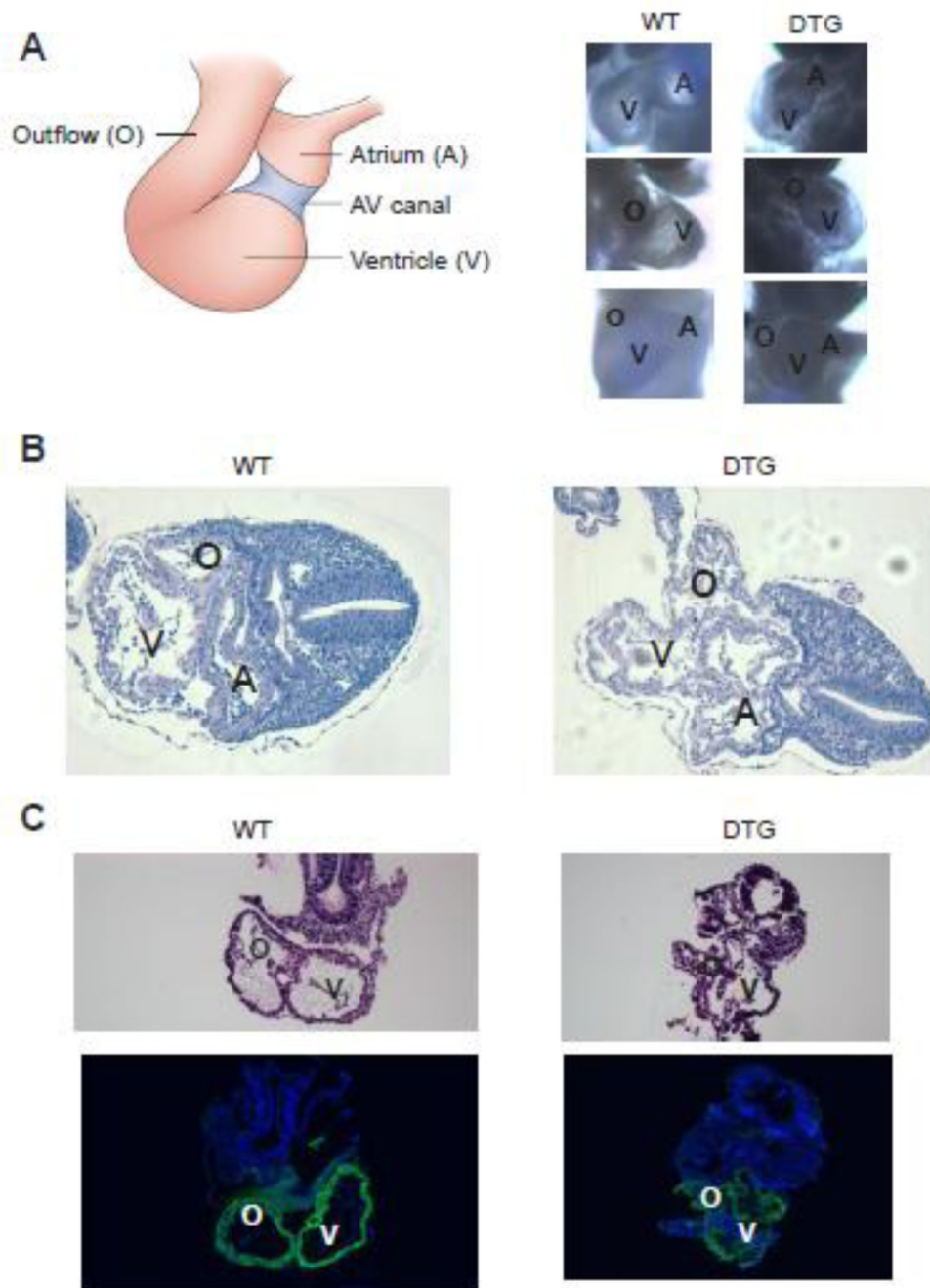


Figure 5. DTG embryos demonstrate normal looping pattern

(A) Left: Schematic frontal view of 9.5 dpc looped heart. Right: Bright field images of 9.5 dpc WT and DTG embryos demonstrate normal looping pattern. Upper panel: left lateral view. Middle panel: right lateral view. Lower panel: frontal view. A=atrium, V=ventricle, O=outflow. (B) H&E staining of transverse sections of 9.5 dpc WT (left) and DTG embryos. Note that although looping pattern was normal, DTG embryos demonstrate collapse of all cardiac structures. A=atrium, V=ventricle, O=outflow. (C) H&E staining of sagittal sections of 9.5 dpc WT (left) and DTG. Lower panel demonstrates positive immunostaining (green)

for α -smooth muscle actin (α -SMA), a marker of early cardiac mesoderm, in both WT and DTG. V=ventricle, O=outflow.

Table 1

K_{ATP} currents in embryonic myocytes

K_{ATP} currents (number of cells (#) and current density), as assessed by whole cell recordings, at different developmental stages (9.5–17.5 dpc) in the WT and overexpressed STG embryonic cardiomyocytes. n represents number of embryos. N represents number of pregnancies. K_{ATP} positive cells (using cutoff value of <0.5 pA/pF as lack of K_{ATP}), demonstrated either basal (immediately after breaking in), spontaneously activating (without pinacidil exposure), or as a result of pharmacologic activation by pinacidil and inhibition by glibenclamide. Cells that demonstrated no K_{ATP} even after exposure to pinacidil for > 60 seconds, were designated K_{ATP}-negative cells. Cells that did not demonstrate K_{ATP}, but were exposed to pinacidil for less than 60 seconds were designated as undetermined (UD).

Genotype	KATP positive cells	KATP Negative cells	Basal/spontaneous KATP # of cells (Basal current density, pA/pF)	Peak KATP # of cells (Peak current density, pA/pF)	UD cells	Total n/N
WT	11	15	7 (1.4±0.6)	26 (11.2±5)	50	76/10
Line 4	13	6	6 (5.8±2.9)	19 (10.6±3.3)	19	38/7
Line 720	0	4	0	0	12	16/3